Role of Effective Composition on Dynamics of PEO−PMMA Blends

Javier Sacristan, Chunxia Chen, and Janna K. Maranas*

Department of Chemical Engineering, The Pennsylvania State University, University Park, Pennsylvania 16802

Received February 14, 2008; Revised Manuscript Received May 14, 2008

ABSTRACT: We use molecular simulation to compare component dynamics of a poly(ethylene oxide) [PEO] and poly(methyl methacrylate) [PMMA] blend with that of a diblock copolymer of the same overall composition. The blend and the copolymer have different intermolecular packing, which leads to a difference in compositions defined over local length scales. These "effective concentrations" directly impact dynamic behavior through the chain connectivity model for blend dynamics, which is based on a single controlling length scale for dynamics equal to the Kuhn length. By comparing the change in dynamics expected on the basis of different effective concentrations with the actual change observed in the simulations, we find that this idea is quantitatively accurate for the PMMA component. For PEO, the controlling length scale for dynamics varies with the size of the observation volume.

Introduction

Blending polymers to form a mixture introduces new materials with desired properties, is simple and inexpensive, and does not require polymerization of new monomers. Material properties of blends often depend directly on composition; the resulting ability to fine-tune properties is an attractive feature of blends in applications ranging from controlled drug delivery systems to new packaging materials. Many important material properties depend on molecular mobility: examples include viscosity, diffusion, and the kinetics of phase separation. Unfortunately, molecular mobility does not depend on composition in a simple and predictable manner. For example, the dynamic responses of the components in a miscible polymer blend are distinct from one another,[1,2] different from the respective pure states,[3] and broader than those of a single-component system.[4] Understanding and predicting the mobility of each component, and ultimately macroscopic blend properties, is an important scientific issue.[5]

Two of the models developed for this purpose are based on the idea of a local volume relevant to dynamics, within which the composition differs from the macroscopic or bulk value. In the concentration fluctuation model,[3,6,7] the local composition differs from the bulk value because of fluctuations related to thermodynamics. The magnitude of these fluctuations depends on proximity to the critical point and depends on component molecular weights, the use of deuterium labels, and the interaction parameter, χ. The relevant dynamic length scale is the cooperative volume as described by Donth for the glass transition.[8,9] This varies but can be regarded as on the order of 10−30 nm. In the chain connectivity model,[10] the local composition differs from the bulk value because of covalent bonding along the chain backbone. In this case, the controlling volume for dynamics is the Kuhn length, l_k, of each component, on the order of 10 Å. This volume is sufficiently small that chain connectivity will significantly alter its composition compared to bulk values. In what follows we consider two systems in which the local composition varies over length scales of 5−25 Å, while keeping other system variables [bulk composition, identities of the two components] constant. This is accomplished by comparing a blend of two homopolymers with a diblock copolymer in which the same two polymers form the two blocks, with lengths that result in the same overall composition. We use molecular simulation, with which the local composition is easily characterized as a function of length scale. Because of the small size of the simulated chains, concentration fluctuations related to thermodynamics are minimal, thus isolating the role of local composition arising from local packing and connectivity. The two systems present different intermolecular packing, resulting in different values of the local composition throughout the length scales mentioned above. These length scales are not relevant to concentration fluctuations but provide a useful test of the chain connectivity model. Specifically, it will address the question of the appropriate controlling length scale for mixture dynamics.

In the chain connectivity model, the local composition of each component is defined via an "effective" concentration:[10]

$$\phi_{\mathrm{eff}}^{\mathrm{A}} = \phi_{\mathrm{self}}^{\mathrm{A}} + (1 - \phi_{\mathrm{self}}^{\mathrm{A}})\phi_{\mathrm{bulk}} \tag{1}$$

that consists of two terms. The first represents contacts within the same chain and is quantified by the "self concentration":

$$\phi_{\mathrm{self}}^{\mathrm{A}} = \frac{C_\infty M_0}{\kappa \rho N_{\mathrm{A}} V} \tag{2}$$

where C_∞ is the characteristic ratio, M_0 the molecular mass of the repeat unit, k the number of backbone bonds, ρ the density, and N_{A} Avogadro's number. This expression is based on counting self contacts within a cubic volume with sides equal to one Kuhn length, thus introducing that length scale to the model. In principle, ϕ can be predicted on the basis of properties of the pure component of interest but in practice is often regarded as a fit parameter. The second term in eq 1 represents contacts with other chains, where it is assumed that these intermolecular contacts are governed by the bulk composition.

The second part of the model connects this effective concentration to segmental relaxation times by means of the Vogel−Tamman−Fulcher (VTF) equation:

$$\tau_{\mathrm{seg}}^{\mathrm{A}}(\phi_{\mathrm{eff}}^{\mathrm{A}}, T) = \tau_{\infty,\mathrm{A}} \exp\left[\frac{B_{\mathrm{A}}}{T - T_{0,\mathrm{A}}(\phi_{\mathrm{eff}}^{\mathrm{A}})}\right] \tag{3}$$

Here B_{A} and $\tau_{\infty,\mathrm{A}}$ are the VTF parameters that describe the temperature dependence of the characteristic relaxation times for the pure components. The effective concentration enters via the effective Vogel temperature:

* Corresponding author. E-mail: jmaranas@engr.psu.edu.

10.1021/ma8003373 CCC: $40.75
Published on Web 06/21/2008

$$T_{0,A}(\phi_{eff}^{A}) = T_{0,A} + [T_{g,eff}^{A}(\phi_{eff}^{A}) - T_g^{A}] \quad (4)$$

where $T_{0,A}$ is the Vogel temperature for pure A. The effective glass transition temperature $T_{g,eff}^{A}(\phi_{eff}^{A})$ must be predicted or measured and is often assigned based on the Fox relation:

$$\frac{1}{T_{g,eff}^{A}} = \frac{\phi_{eff}^{A}}{T_g^{A}} + \frac{1-\varphi_{eff}^{A}}{T_g^{B}} \quad (5)$$

where T_g^{A} and T_g^{B} are the glass transition temperatures of the pure components. This model successfully describes the temperature and composition dependence of dynamics in many miscible blends: examples include poly(isoprene)/poly(vinylethylene) (PI/PVE),[11] blends formed from different saturated hydrocarbons,[12–14] poly(vinyl methyl ether)/polystyrene (PVME/PS),[2] and in 1,4-polyisoprene/1,2-polybutadiene[15] and PS/PI diblock[16] and tetrablock[17] copolymers.

The purpose of this work is to investigate the relationship between the effective concentration and dynamics in poly(ethylene oxide) [PEO]/poly(methyl methacrylate) [PMMA] homopolymer and diblock copolymer blends through molecular dynamics simulation. Computer simulation is a powerful tool to directly investigate the static and dynamic features of polymer systems.[12,13,18,19] In this case, molecular dynamics simulation allows us to measure both ϕ_{eff} and ϕ_{self}, neither of which is accessible experimentally, and to monitor the resulting dynamics as a function of local volume size. This allows us to establish a direct connection between ϕ_{eff} and the characteristic relaxation time. In order to isolate the effect of the effective concentration on dynamics, we investigate mobility as a function of position along the chain backbone, taking into account the influence of the junction point and chain ends on mobility. After eliminating those atoms where dynamics are directly influenced by chain position, we ask if the chain connectivity model is able to predict the difference in mobility between the two systems from the difference in effective concentrations.

Simulation Details

Model. We simulate two systems, both of which contain 20 wt % PEO and 80 wt % PMMA: a blend of the two homopolymers and a diblock copolymer. The former is a mixture of two different chains, while in the latter, the two materials are combined in a single chain. The simulation box for the blend contains 42 chains of PMMA and 8 chains of PEO. The PEO chains, $CH_3-[-CH_2-O-CH_2-]_{30}-CH_3$, have 30 repeat units and a molecular weight of 1350 g/mol, while the PMMA chains, $CH_3-[CCH_3COOCH_3-CH_2]_{10}-H$, have 10 repeat units and a molecular weight of 1016 g/mol. In order to form the diblock copolymer, we begin with the 10 repeat unit PMMA chain and add a PEO block of length constrained by the desired composition [5 repeat units]. Conceptually the PEO chains in the blend simulation box are cut, and a piece is placed on the end of the unaltered PMMA chains. The resulting system consists of 25 such chains, each with a molecular weight of 1250 g/mol, with 19% contributed by PEO and 81% by PMMA. For both the blend and the diblock simulations, the united atom formalism (UA) is used, where the force sites represent C, O, CH, CH_2, and CH_3. The force fields for this purpose are obtained from refs 20 and 21. We have previously considered both pure PEO[22] and pure PMMA,[23] and complete discussions of the force fields used for each can be found in those references. These references also contain detailed comparisons to existing experimental data showing that the force fields for both are realistic. All simulations are performed in the NVT ensemble. We maintain the temperature at 450 K using the velocity rescaling algorithm of Berendsen et al.[24] and select the mixture volume using the densities of the pure components at 450 K and 1 atm assuming no volume changes on mixing. We note that the simulation temperature, 450 K, does not allow to investigate either a decoupling of the dynamics of PEO and PMMA or a suggested confined-like dynamics for PEO observed recently by neutron scattering and molecular dynamic simulations on a PEO/PMMA homopolymer blend at low temperature.[25]

The cutoff distance for nonbonded interactions is 8 Å, and the Ewald summation method[26,27] is used to calculate long-range Coulomb interactions. To decrease computation time, we employ the multiple time step reversible reference system propagator algorithm, rRESPA,[28,29] with timesteps of 1 fs for bonding, bending, and torsions, 2 fs for van der Waals and the real part of the Coulomb Ewald summation, and 4 fs for the reciprocal contribution to the Coulomb Ewald summation.

To prepare the initial simulation boxes, identical copies of the required chains are placed in a box large enough to prevent chain overlap. Homopolymer single-chain configurations are generated by a pivot Monte Carlo sampling procedure. Diblock copolymer single-chain configurations are obtained starting with the relaxed PMMA homopolymer chains and adding the PEO block as described above. This block is taken from a relaxed PEO chain, and the joined chain is not subjected to further pivot Monte Carlo relaxation. In the initial phase of the simulation, the box size is gradually decreased to the appropriate value: cubic boxes with sides of 36.5 Å for the copolymer and 42.4 Å for the blend. The resulting box sizes are greater than $4R_g$ in all cases.

The properties of interest in this work are segmental relaxation times obtained from the self intermediate scattering function, effective concentrations over spatial scales from 2 to 20 Å, and intermolecular pair distribution functions. As such, the most important criteria for equilibration are that these properties do not drift with time. We also require that, at a minimum, the slowest component PMMA has traveled a distance equal to its R_g during the equilibration period. On this basis, we choose equilibration times of 4 ns for the blend and 3 ns for the copolymer. The lack of drift following these equilibration periods is illustrated in Figure 1, where we plot two quantities: the effective concentration of PEO in the blend simulation over 2 ns blocks and the self intermediate scattering function, $F_i(Q = 1\ \text{Å}^{-1}, t)$, of all atoms in the copolymer simulation over 3 ns blocks. No variations in block averages are observed over the duration of the production runs.

Results and Discussion

Structure and Chain Packing. In the chain connectivity model,[10] the dynamic response of each component is influenced by a self enrichment of the local environment that derives from intramolecular connectivity. We expect this enrichment will differ between the blend and copolymer systems. In order to quantify it directly from our simulations, we calculate the self and effective concentrations:

$$\Phi_{self}^{A}(r) = \left\langle \frac{N_{A,intra}(r)}{N_A(r) + N_B(r)} \right\rangle \quad (6)$$

$$\Phi_{eff}^{A}(r) = \left\langle \frac{N_A(r)}{N_A(r) + N_B(r)} \right\rangle \quad (7)$$

where r is the radius of a sphere within which the self concentration is determined, $N_{A,intra}(r)$ is the number of A atoms on the same chain as a reference A atom, and $N_A(r)$ and $N_B(r)$ are the total number of A and B atoms. Physically, the calculation corresponds to considering a central atom, counting either atoms on the same chain [self] or atoms of the same type on any chain [effective] within a given volume, and dividing by the total number of atoms within that volume. The results are averaged over all atoms in the system by regarding each atom in turn as the center atom, indicated by the brackets. In

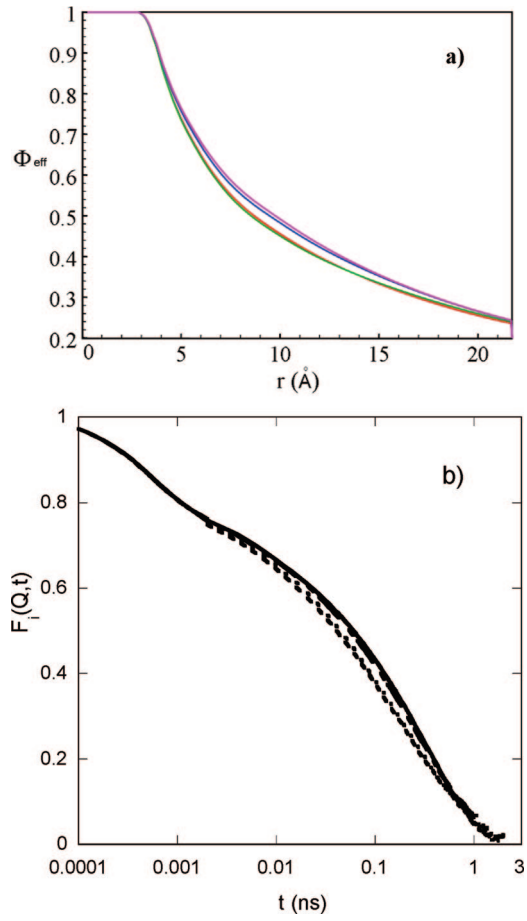

Figure 1. (a) Effective concentration of PEO in the blend simulation over 2 ns blocks, different curves represent consecutive 2 ns blocks. (b) Self intermediate scattering function at $q = 1.0$ Å^{-1} of all atoms in the copolymer simulation calculated over 3 ns blocks; different curves represent 3 ns consecutive blocks.

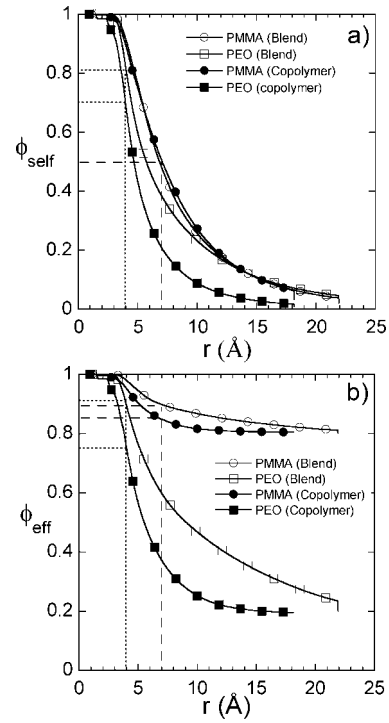

Figure 2. Differences in self (a) and effective (b) concentrations of PEO and PMMA between blend and copolymer systems as a function of local volume size. Dashed lines correspond to the averaged concentration at the Kuhn length, $r = l_k/2$, of each polymer. Long dashes: PMMA. Short dashes: PEO.

Table 1. End-to-End Distance, R_e, and Gyration Radius, R_g, of PEO and PMMA in the Copolymer and in the Blend

	R_g^{blend} (Å)	R_e^{blend} (Å)	R_g^{cop} (Å)	R_e^{cop} (Å)
PEO	9.5	21	4.1	10.8
PMMA	6.8	16.5	6.3	14.7
PEO−PMMA			7.5	18.9

the original reference, the shape of the local region is a cube,[10] whereas we use a spherical volume to correspond more directly with the spatial selectivity in the self intermediate scattering function, with which we will assess dynamics below. This may cause differences in the numerical values of the self or effective concentrations from other published results but does not alter the physical basis of the model.

In Figure 2 we plot the self and effective concentrations of PEO and PMMA in both systems as a function of local volume size. We indicate the radius, $r = l_k/2$, that corresponds to the Kuhn lengths of each component with vertical lines. The Kuhn length of PEO is 8 Å,[30] and the Kuhn length of PMMA is 14 Å.[30] The self concentrations plotted in Figure 2a are unity at short distances where intermolecular contacts are not possible and fall off to zero as the end-to-end distance is approached (see Table 1 for end-to-end distances). Effective concentrations plotted in Figure 2b also are unity at short distances and fall off to the bulk concentration, which by definition must be recovered when the spatial scale reaches half the simulation box. The spatial scale at which either concentration begins to decrease from unity is artificially extended in our case due to the use of a united atom model, which does not have the closer intermolecular contacts that would result from hydrogen atoms. The blend case would clearly benefit from simulations on a larger system because the effective concentrations have not plateaued at the bulk concentration before the influence of the simulation box size intervenes. As a result, it is possible that the effective concentrations in the PEO/PMMA blend remain above the bulk concentration for longer than we are able to ascertain.

The self concentration of PMMA is not sensitive to the type of system: the copolymer and blend curves are coincident. In contrast, the self concentration of PEO decays more rapidly with local volume size in the copolymer than in the blend. This behavior can be explained on the basis of chain dimensions of both components presented in Table 1. The number of intramolecular contacts, and thus the self concentration, will reach zero near the end-to-end distance for each component in each system. Since we prepared the copolymer system to have the same bulk concentration as the blend by covalently bonding small pieces of PEO to the exact PMMA chains used in the blend simulations, the end-to-end distances of PMMA are similar between the blend and the copolymer, but those of PEO are quite different. Specifically, the end-to-end distance of PEO in the copolymer is considerably smaller than PEO in the blend or either of the PMMA systems. As a result, the self concentration of PEO in the copolymer should drop off to zero more rapidly than any of the other three cases, and this behavior is reflected in Figure 2a.

The variation of effective concentration with local volume size is illustrated in Figure 2b. It is clear that for a given local volume size the effective concentrations of both PEO and PMMA are smaller in the copolymer than in the blend. The effective concentration reflects both intramolecular and intermolecular packing of like species, either of which can vary between the copolymer and the blend systems. As shown in Figure 2a, the self concentration and therefore the intramolecular

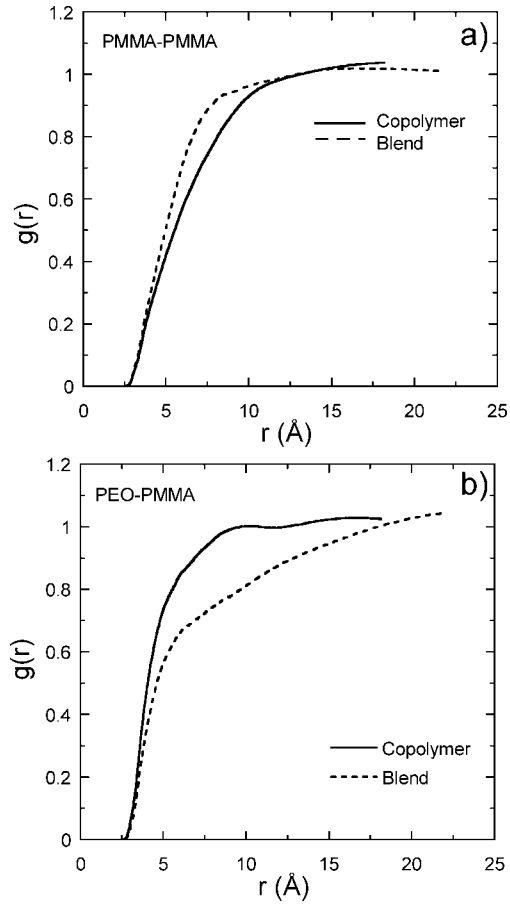

Figure 3. Intermolecular packing of PMMA in the blend and copolymer systems: (a) the PMMA−PMMA intermolecular pair distribution function; (b) the PEO−PMMA intermolecular pair distribution function. Dotted lines: blend. Continuous lines: copolymer.

contribution do not differ between the two systems for PMMA. As a result, differences in the effective concentration must arise from changes in intermolecular packing between the two types of systems. We cannot make a similar statement for PEO, as differences in self concentration between the blend and copolymer systems are evident in Figure 2a.

To investigate differences in intermolecular packing between the blend and the copolymer as a cause for the observed differences in the effective concentration, we consider various intermolecular pair distribution functions for the two systems in Figure 3. Three types of distributions are possible: PMMA−PMMA, PEO−PMMA, and PEO−PEO. To establish the role of intermolecular packing in the effective concentration for PMMA, we consider differences in self packing [PMMA−PMMA] and packing with PEO [PEO−PMMA] between the two systems. We do not make the same comparison for PEO because as the minority component, statistics for the PEO−PEO distribution are poor. The PMMA−PMMA distribution is higher in the blend than in the copolymer, whereas the opposite is true for the PEO−PMMA distribution. This suggests that in the copolymer PMMA packs less efficiently with itself and more efficiently with PEO, consistent with the reduced effective concentration. This allows us to conclude that the decrease in effective concentration between the blend and the copolymer is a consequence of a change in intermolecular packing. We cannot make a similar statement for PEO because the self concentration changes, and as mentioned above, no conclusions may be drawn from the PEO−PEO distribution.

The larger value of ϕ_{bulk} for PMMA compared to PEO makes it difficult to assess how quickly the effective concentrations

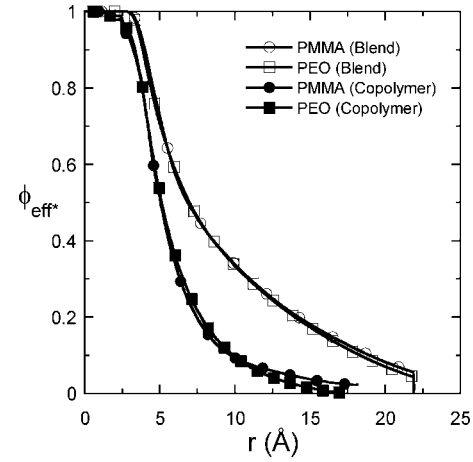

Figure 4. Normalized effective concentrations as a function of the volume size. PEO: squares. PMMA: circles. Filled symbols: copolymer. Unfilled symbols: blend.

of each approach their bulk values. In order to eliminate this difficulty, we normalize the effective concentration: $\phi^*_{eff} = (\phi_{eff} - \phi_{bulk})/(1 - \phi_{bulk})$, so that it varies between zero and unity. At short distances where the effective concentration is unity, the normalized effective concentration is also unity, but as ϕ_{eff} approaches the bulk concentration, the normalized effective concentration approaches zero. These normalized effective concentrations are plotted in Figure 4 for both components, from which it is apparent that the effective concentrations of PEO and PMMA decrease toward their respective bulk values in exactly the same way. Although this decrease is invariant between components in the same system, a difference between the blend and copolymer systems remains evident: the effective concentrations decrease toward the bulk concentration faster in the copolymer than in the blend. When placing PMMA in a block copolymer with PEO, rather than mixing with separate PEO chains, the self concentration is invariant. The effective concentration of PMMA changes significantly and is associated with changes in intermolecular packing. PEO, when incorporated in a block copolymer with PMMA, alters its self concentration. However, this appears to have a negligible influence on the effective concentration: if it were significant, then the normalized effective concentrations of PEO and PMMA in the copolymer would differ.

When going from a blend to a copolymer, the effective concentration can be influenced not only by different packing but also by a reduction in self contacts because the atoms at the junction point will have connections with atoms of the same type replaced with connections to the other component. This effect may extend for several atoms surrounding the junction point. To eliminate the possibility that these atoms significantly alter the averages discussed above, we have considered the effective concentration as a function of atom position and compare it to the average values reported in Figure 2b. There are three PMMA atoms and one PEO atom surrounding the junction point with effective concentrations that differ significantly from the average value. We remove these atoms from consideration in further calculations and note that the resulting difference in effective concentration is small. This adjustment does not influence our prior conclusion as at any given length scale $\phi^*_{eff,PEO}$ and $\phi^*_{eff,PMMA}$ remain smaller in the copolymer than in the blend.

Between the two types of PEO/PMMA mixtures we have considered, a blend and a diblock copolymer with the same PEO content, the effective concentrations differ. We now consider the distribution of effective concentrations about the values discussed in Figure 2. Each point in Figure 2 represents an

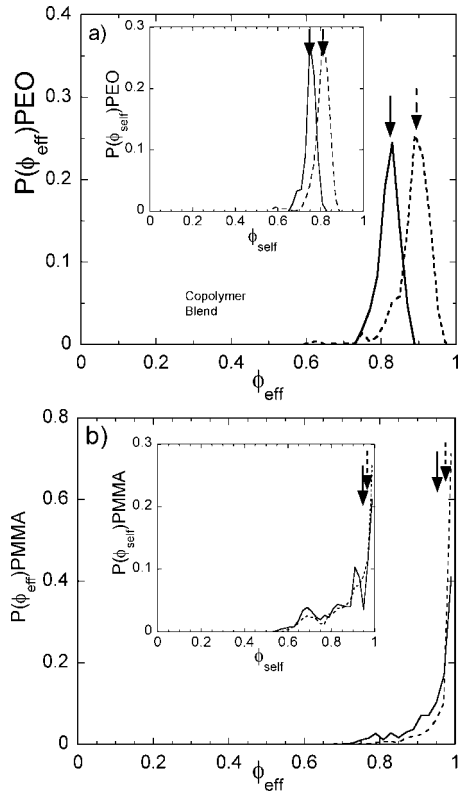

Figure 5. Distribution of effective [main graph] and self [inset] concentrations at the Kuhn length of PEO: (a) PEO; (b) PMMA. Continuous lines: copolymer. Dashed lines: blend. Arrows indicate the average values of both quantities reported in Figure 2.

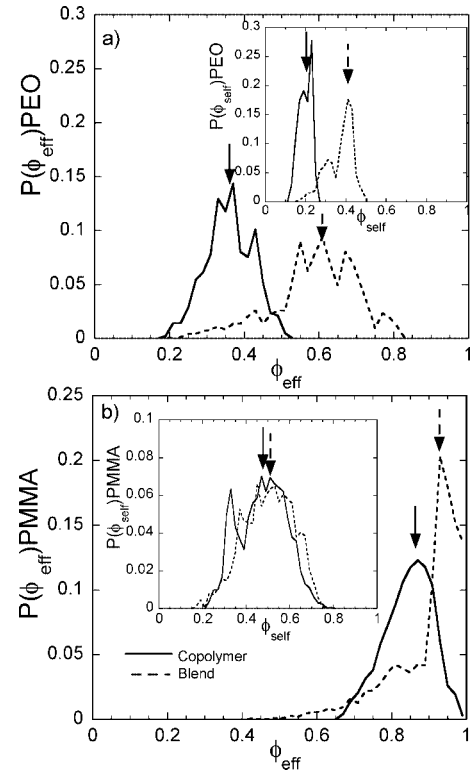

Figure 6. Distribution of effective [main graph] and self [inset] concentrations at the Kuhn length of PMMA: (a) PEO; (b) PMMA. Continuous lines: copolymer. Dashed lines: blend. Arrows indicate the average values of both quantities reported in Figure 2.

average, at a given spatial scale, over all the atoms in the system. Underlying this average is a distribution of local compositions, the width of which may also influence mobility. We consider the probability distributions of effective and self composition at two spatial scales: the Kuhn lengths of PEO and PMMA. These two spatial scales are indicated in Figure 2 by dashed lines. The Kuhn length of PEO is 8 Å,[30] which corresponds to a sphere with a radius of 4 Å. Probability distributions for both components at this spatial scale are presented in Figure 5. As mentioned above, those atoms that are directly influenced by the junction point are not included. The distribution of effective concentrations is displayed in the main figure, while the inset provides the distribution of self concentrations. The average values of both quantities reported in Figure 2 are indicated by arrows. At this small spatial scale, the distributions for both components are narrow, and their width does not differ between the blend and the copolymer. Differences in the average values are evident only for PEO, as expected on the basis of Figure 2. Probability distributions at the spatial scale corresponding to the Kuhn length of PMMA, 14 Å,[30] are presented in Figure 6. It is immediately obvious that at this larger length scale the distributions of both self and effective concentrations are wider than at the Kuhn length of PEO. The distribution of self concentrations for the PMMA component is similar in the blend and copolymer—both with respect to the average value and the width. For the PEO component, both the width and the average value of the self concentration differ between the two systems. Specifically, the distribution in the copolymer is narrower, suggesting that the atoms in that system experience less variation in their local environments than the same atoms in the blend. For both PEO and PMMA, the distribution of effective concentrations is wider and more asymmetric in the blend than in the copolymer. Again, this indicates that at $r = 7$ Å atoms in the blend sample a wider range of environments than their counterparts in the copolymer sample.

At the Kuhn length of PMMA [Figure 6], the widths of the blend and copolymer effective concentration distributions differ, whereas this is not the case at the Kuhn length of PEO [Figure 5]. The average values of the effective concentrations differ at both length scales. This variation in behavior, specifically that at the Kuhn length of PEO the average values differ while the widths remain the same, whereas both quantities differ at the Kuhn length of PMMA, provides an opportunity to test whether the details of the distribution influence dynamic response. If we accept that the Kuhn length is the controlling length scale for dynamics and if the average value of the effective concentration adequately captures dynamic behavior, then for both components dynamic properties will be predicted accurately by the chain connectivity model which requires these average values at their respective Kuhn lengths. Differences in predictive capability, specifically if PEO is predicted accurately but PMMA is not, would indicate that details of the distribution are important.

Mobility and Dynamics. We now turn our attention to the dynamic properties of the two systems. Our objective is to determine whether differences between blend and copolymer segmental relaxation times can be predicted on the basis of differences in effective concentration discussed above. The changes between blend and copolymer effective concentrations will influence dynamics if the relevant length scale for dynamics lies within the range where they differ: 5−20 Å. In this case, dynamic behavior of each component will be more influenced by the presence of the other in the copolymer than in the blend. This expectation is supported by the atomic mean-squared displacements, MSD, presented in Figure 7 for both components in the two systems. At any time, the difference between the average distance moved by PEO and PMMA atoms in the copolymer is smaller than the same difference in the blend. Thus, the smaller effective concentrations of both components in the copolymer are reflected in mobility as assessed by the MSD.

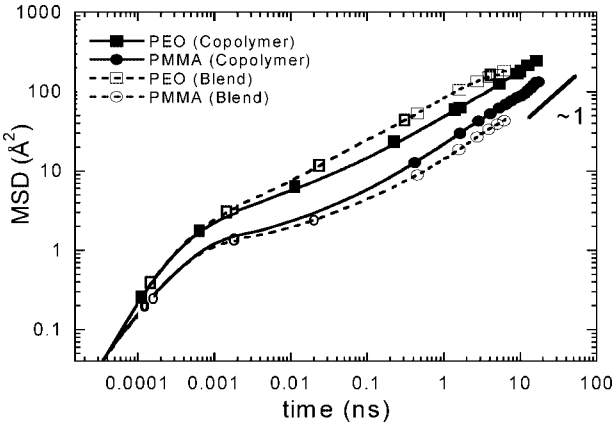

Figure 7. Comparison of component mobility in the blend and copolymer systems. Mean-squared displacements are shown for PEO [squares] and PMMA [circles] in both systems. Filled symbols: copolymer. Unfilled symbols: blend.

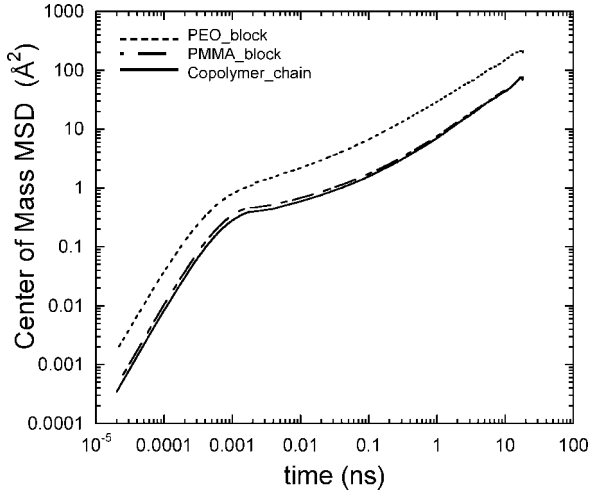

Figure 8. Chain mobility of the copolymer and its individual blocks as assessed by the center-of-mass mean-squared displacement. Continuous line: entire copolymer chain. Dotted line: PEO block. Dashed line: PMMA block.

The decrease in effective concentration acts to retard mobility of PEO atoms compared to the blend system, whereas it accelerates mobility of PMMA atoms. Because the PEO and PMMA blocks are directly connected, we expect that the MSD, at long enough times, will be coincident for both blocks. This behavior is not observed for the atomic MSD, within the time scale of our simulations. We can examine this behavior by considering the center-of-mass MSD, presented in Figure 8, which characterizes chain, rather than atomic, mobility. The center-of-mass MSD of the entire copolymer follows that of the PMMA block, while the PEO block is significantly faster. The mobility of the entire copolymer chain is thus controlled by the slowest block, PMMA.

As with the effective concentration, we wish to identify those atoms whose mobility is directly influenced by proximity to the junction point in the copolymer. Atoms whose mobility is altered for this reason should be excluded when relating dynamic properties to effective concentration. Chain end effects are the only mechanism for varying mobility in the blend components: they are evident within 2 Å [PMMA] or 4 Å [PEO] of the chain ends. In the copolymer, chain end effects are present along with the influence of the junction point. For PMMA, mobility is influenced by the faster PEO for a distance of 3 Å from the junction point. This is separated from chain end effects by a region in which mobility does not vary with chain position. Mobility of the PEO segment increases with distance from the junction point, but because it is short, this increase overlaps that from chain end effects. Since they both act to increase PEO mobility, we cannot distinguish one from the other and remove its influence. In what follows, we remove the effect of the junction point for PMMA by disregarding atoms within 3 Å of the junction point. This criterion is met by disregarding the three atoms for which the effective concentration is influenced by the junction point as described above. For PEO, we eliminate the one atom where effective concentration is influenced by the junction point. As we cannot identify atoms in which mobility is directly impacted by the junction point, we do not attempt to remove them. This must be taken into consideration when interpreting our results. The end atoms are not removed from consideration because differences in mobility due to chain ends influence the copolymer and blend systems in the same way.

We now consider the link between segmental relaxation times and effective concentration by using the chain connectivity model to correlate observed differences between the two systems. Segmental relaxation times are assessed via the self intermediate scattering function, $F_i(Q,t)$, where $Q = 2\pi/r$ represents the spatial extent of mobility. This function may be measured experimentally using the incoherent contribution to quasi-elastic neutron scattering and is related to the atomic displacements of single atoms. The self intermediate scattering function quantifies the correlation of atomic positions over a time interval t:

$$F_i(Q,t) = \frac{1}{N}\sum_{i,j} \frac{\sin Q[r_i(t_0+t) - r_i(t_0)]}{Q[r_i(t_0+t) - r_i(t_0)]} \tag{8}$$

where $r_i(t)$ is the position of the atom at time t and $r_i(t_0)$ at a reference time t_0. The self intermediate scattering functions of the copolymer and blend systems are compared in Figure 9 as a function of spatial scale. The spatial scales chosen vary from typical intramolecular separations, [$Q = 2.0$ Å^{-1} or $r = 3.14$ Å] to chain dimensions [$Q = 0.37$ Å^{-1} or $r = 17$ Å]. The lowest Q value corresponds to distances less than half the periodic box in all cases.

The spectra are characterized by a two-step decay as reported previously for other polymers.[31,32] Note that because we use a united atom model, the rotation of methyl groups is not present for the PMMA component. The distinction between the fast [times less than 1 ps] and slow [times longer than 1 ps] parts of the decay is more pronounced in PMMA than in PEO. In addition, the fast process in PEO decays significantly further before the slower process intervenes, probably because the lack of side groups allows PEO atoms to explore a larger region[33] and because the effective glass transition temperature of PEO is higher than that of PMMA in both systems. The origin of the fast process is related to movement within a restricted area or local "cage". Supporting this observation, it is not influenced by environment:[34] the fast decay is insensitive to whether the material is blended or incorporated in a copolymer.

The slower decay corresponds to the structural or α-relaxation and depends on the type of system: in the copolymer, PMMA atoms move faster and PEO atoms slower, consistent with the MSDs and the expectation that the smaller effective concentrations in the copolymer will lead to less separation in component dynamics. These observations are common to all spatial scales; however, the size of the separation between the two systems is relatively constant for PMMA, whereas it is a strong function of Q for PEO. As the physical difference encountered with varying Q is the size of the region over which dynamics is observed, a continuously increasing separation as Q is decreased means that the extent to which dynamics of PEO are influenced depends on the size of the observed region, which is not consistent with the idea of a single length scale that controls

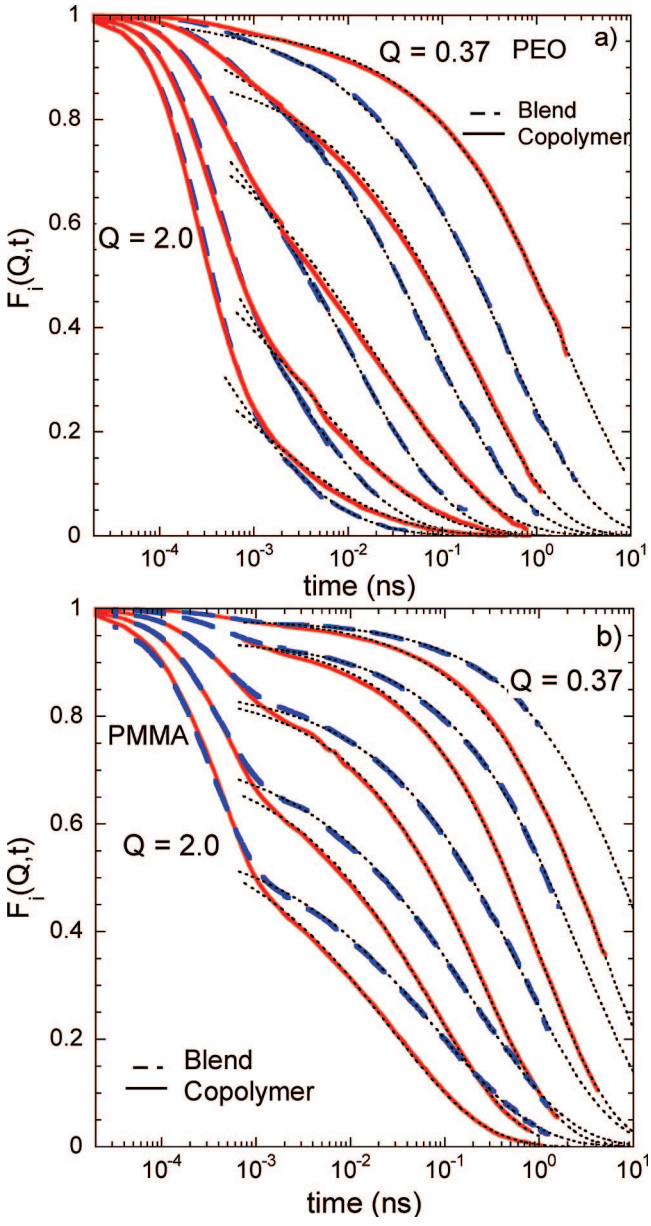

Figure 9. Self intermediate scattering function as a function of spatial scale: $Q = 0.37$, 0.6, 1.0, 1.5, and 2.0 Å^{-1}. (a) PEO; (b) PMMA. Dashed lines: blend. Continuous lines: copolymer. Dotted lines: stretched exponential fits.

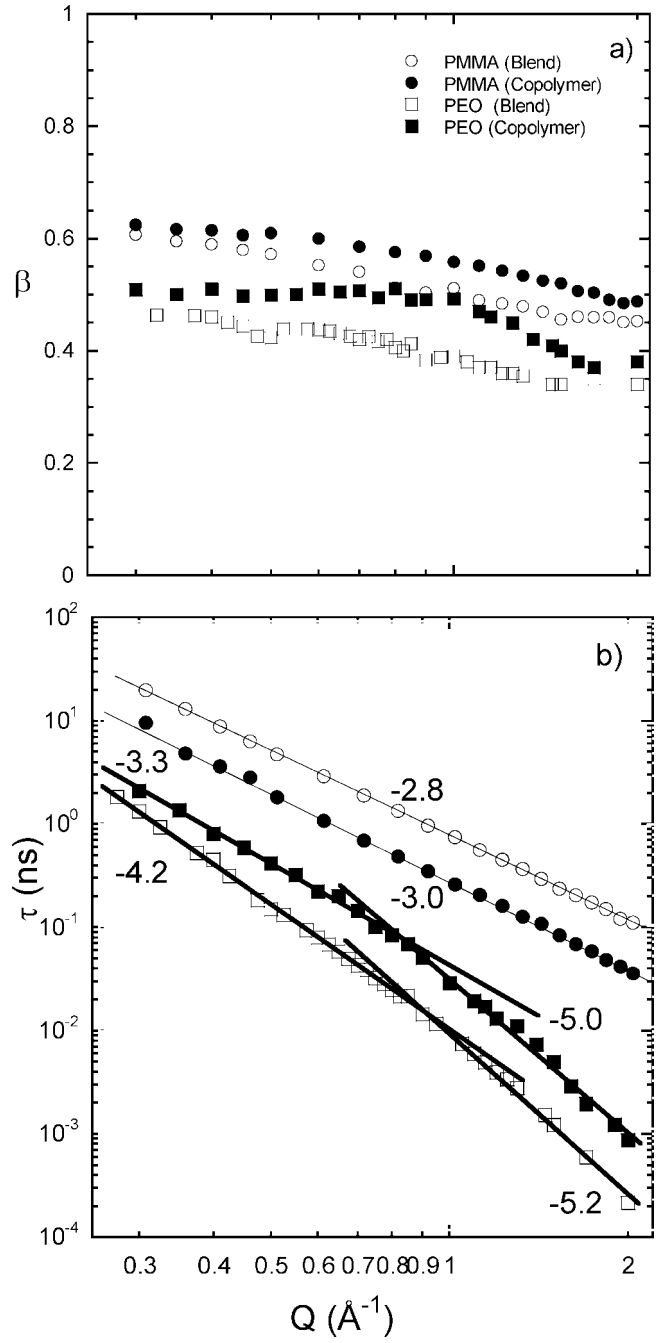

Figure 10. KWW fit parameters as a function of spatial scale: (a) stretching parameter, β; (b) KWW relaxation times, τ. PEO and PMMA are fit separately in both systems. Solid symbols: blend. Filled symbols: copolymer. Squares: PEO. Circles: PMMA.

dynamic response. On the other hand, for PMMA the difference between the two systems is insensitive to spatial scale, in which case the local environment on a single length scale, the Kuhn length for example, may be sufficient to explain the observed differences.

To quantify the differences evident in Figure 9, we employ a fitting procedure for the slow part of the decay; specifically, the empirical Kolraush−Williams−Watts[35] (KWW) expression is used for this purpose:

$$F_i(Q,t) = A(Q,T)\exp\left[-\left(\frac{t}{\tau(Q,T)}\right)^{\beta(Q,T)}\right] \quad (9)$$

This procedure returns an average relaxation time, τ, as a function of spatial scale and temperature and a parameter that characterizes the width of the relaxation time distribution, β, also a function of Q and T. The amplitude $A(Q,T)$ accounts for the initial decay not directly quantified by this fitting procedure. Our methodology in fitting the data to eq 9 is to first fit the data with the most pronounced second decay, $Q = 1.0$ Å^{-1}, with all three parameters floating. This fit allows us to select the appropriate time interval for the second decay and fit all other $F_i(Q,t)$. We also require that $A(Q,T)$ not take unphysical values, $1.0 > A(Q,t) > 0$, and to decrease with increasing Q, which is the expected behavior of the Debye−Waller factor. The resulting fit lines are provided in Figure 9 and illustrate that the KWW expression provides a reasonable description of the data.

The resulting fit parameters are plotted in Figure 10 as a function of spatial scale. The stretching parameters of both components, presented in Figure 10a, are smaller in the blend than in the copolymer. This indicates that relaxation times of PEO and PMMA present a larger distribution when blended than joined in a copolymer. The wider distribution of relaxation times in the blend compared to the copolymer, combined with

the larger distribution of effective concentrations, supports the idea that each local concentration contributes a different mobility. The difference between the stretching parameters of the two systems varies considerably with spatial scale for PEO. The largest difference [about 20%] occurs at a spatial scale about 50% larger than its Kuhn length [$Q \sim 1$ Å^{-1}], whereas at the Kuhn length of PEO [$Q \sim 1.6$ Å^{-1}], the stretching parameters are nearly coincident. The variation is smaller but still present for PMMA. The stretching parameters for PEO are smaller than those for PMMA in both systems, consistent with the distributions of effective concentrations at the Kuhn length of PMMA [$Q \sim 0.9$ Å^{-1}], which are narrower for PMMA (Figure 6). The appropriate comparison, assuming a controlling dynamic length scale equal to the Kuhn length of each component, is between the distribution of PEO in Figure 5a and that of PMMA in Figure 6b. Taking this comparison, it is evident that the dynamic distribution does not follow the correct trend, since the distribution of PEO at its Kuhn length is narrower than the distribution of PMMA at its Kuhn length. This suggests that one of the two components has a dynamic length scale other than its Kuhn length.

We present relaxation times for both components as a function of spatial scale in Figure 10b. Within the spatial range investigated (3−21 Å), and given the small molecular size of the simulated chains, we expect three scaling regimes: at low Q the Rouse regime [$\tau \propto Q^{-4}$] represents whole chain motion, at intermediate Q the segmental regime appears [$\tau \propto Q^{2/\beta}$], and at high Q another regime [$\tau \propto Q^{-2}$] is observed in both polymers and low molecular weight glass-forming systems.[36–38] As a result, two changes in scaling could appear in Figure 10b. The change from segmental to Rouse behavior is often not detectable because the values of β are near 0.5 and because the Rouse regime is not always clearly delineated in the dynamics of polymers.[39–41] For PMMA, no transitions are observed, and the segmental regime, $\tau \propto Q^{-2/\beta}$ with $\beta \approx 0.6$, appears to extend throughout the entire spatial range. Within this regime, which we expect would be well described by the chain connectivity model, characteristic relaxation times are separated by an amount that is independent of spatial scale. This is consistent with the observation that differences in the blend and copolymer decay curves of PMMA do not depend on spatial scale. The invariance of $\tau_{blend}/\tau_{copolymer}$ to spatial scale, taken with the obvious variation between $\phi_{eff,blend}$ and $\phi_{eff,copolymer}$ as local volume size is varied, suggests that a single length scale controls dynamics for PMMA. The lowered effective concentration of PMMA at its Kuhn length in the copolymer system could thus explain the faster motion of this component and will be tested quantitatively below. We remind the reader that atoms influenced directly by the junction point have been omitted from the calculation, and thus these observations reflect the indirect influence of incorporating PMMA into a copolymer: specifically the change in local environment experienced by PMMA atoms.

The situation for PEO is different. A Q-independent difference between the two systems is observed only for spatial scales less than ~7 Å. At larger length scales the difference between the two systems depends on spatial scale. This suggests that although a single length scale may control dynamics of PEO over small distances, the mechanism for motion is different at length scales greater than 7 Å. Because the end-to-end distance of the PEO segment in the copolymer is much smaller than that of the PEO component in the blend, it is possible that in the copolymer PEO enters a Rouse scaling regime, whereas this does not occur in the blend. Although this is supported by the fact that the stretching parameter stops increasing at the spatial scale where the crossover is located, it seems unlikely given that the crossover also appears for PEO in the blend system. It thus appears that this crossover is related to a change in the mechanism of segmental motion from one where a single length scale is appropriate [$Q > 1$ Å^{-1}] to one where the defining length scale changes with the spatial extent over which dynamics is assessed [$Q < 1$ Å^{-1}].

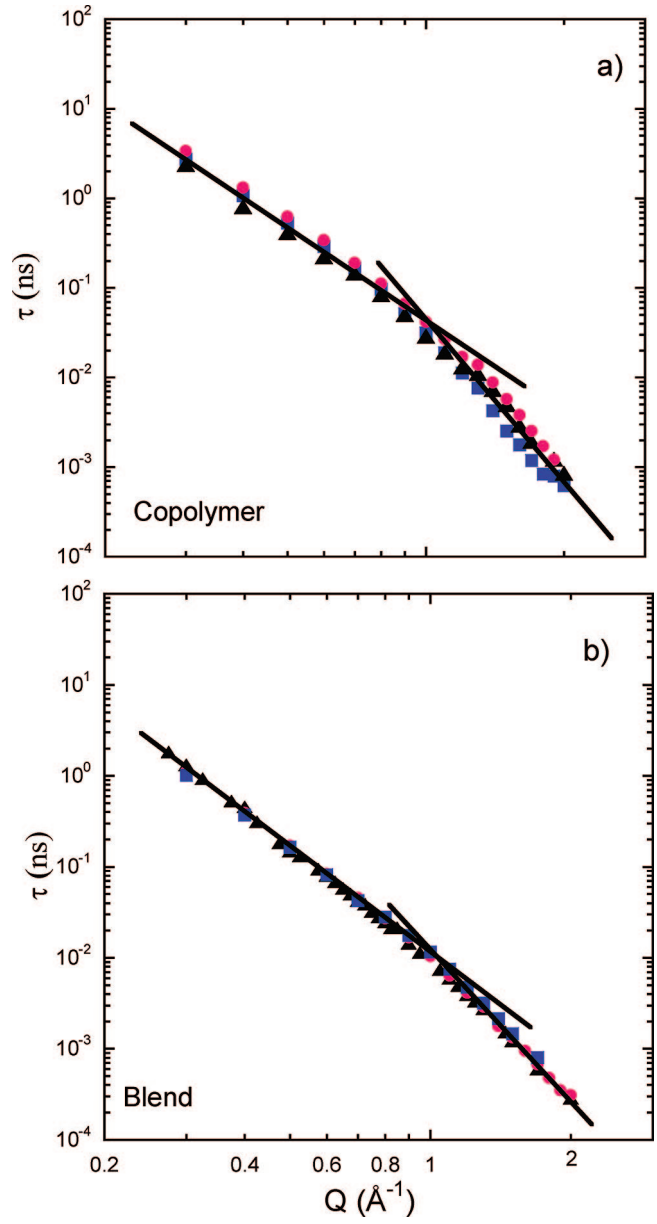

Figure 11. Influence of chain ends on the spatial scaling of relaxation times for PEO: (a) PEO in the copolymer system; (b) PEO in the blend system; (▲) all atoms; (■) all but three end atoms on each chain; (●) all but six end atoms on each chain. For the blend three or six atoms are removed from each chain end.

To test whether this observation is related to chain end effects, we reproduce Figure 10b, omitting those united atoms which differ significantly in mobility because they are located near chain ends. The spatial scaling of relaxation times obtained in this way is illustrated in Figure 11. Variation in mobility with chain position was observed for atoms within 3 Å of the chain ends, and thus we show relaxation times calculated using all atoms, all but the last three atoms, and all but the last six atoms. The data for the blend system are exactly the same, indicating that this change in scaling is not associated with chain end effects. There is more scatter in the copolymer system. This is most likely related to statistics: the copolymer system has roughly half the number of PEO atoms as the blend system, and removing the six end atoms reduces this by ~25%,

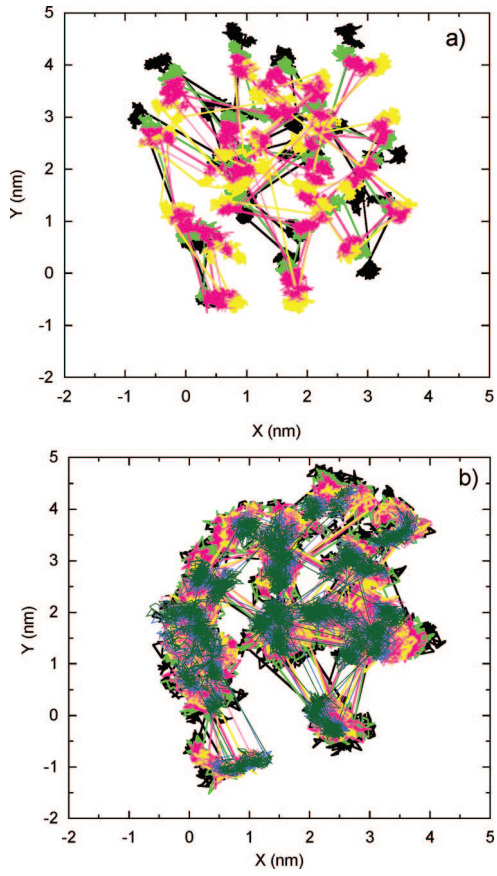

Figure 12. Mechanism of motion in the two components. The movement of (a) PMMA and (b) PEO CH_2 united atoms are represented as position density graphs. Data are plotted every 2 ps over a total duration of 1 ns.

compared to ~15% for the blend. The connection to statistics is also supported by the nature of the variation—the data do not shift continuously with further removal of end atoms, but rather bracket the result obtained using all atoms. Our conclusion is that the change in scaling observed in PEO, but not PMMA, is not an artifact due to end effects.

To gain more insight as to why the mechanisms of motion may differ for PEO and PMMA, we examine the trajectory of six CH_2 united atoms within both PEO and PMMA over 1 ns. In Figure 12, we present position density graphs for these united atoms, plotted every 2 ps over a total of 1 ns. We choose 1 ns as the total time considered because for a characteristic relaxation time of 1 ns PMMA is within the constant offset scaling regime, while PEO is within the regime where the scaling has changed and the offset is no longer constant. Comparison of the two may thus provide information regarding the origin of different scaling behavior. Note that the fast process is ignored by the choice of 2 ps for the choice of plotting interval, as the fast decay (see Figure 9) occurs before $t \sim 1$ ps. For both components, structural relaxation occurs via explorations of local cages punctuated by hopping to new cage locations, consistent with prior observations. There are two differences between the components: the size of the cage and the extent to which cage trajectories overlap. For PMMA the cage size is quite small (2−3 Å), whereas for PEO it is 6−8 Å. The PEO cage size corresponds to the crossover point in the Q scaling of characteristic times: for spatial scales within this size, a constant offset in relaxation times between the two systems (suggesting a single controlling length scale) is observed whereas at spatial scales larger than this the opposite is true. The PMMA cage size corresponds to the smallest spatial scales on the graph, and thus a crossover, should it occur, is not detected. Whereas the trajectories of the PMMA atoms are distinct, with each occupying its own local space without infringement from neighboring atoms, the larger cage sizes in PEO lead to significant overlap of atomic trajectories. Several PEO atoms appear to be sharing the same local cage, with the position of that cage moving throughout the simulation box. In addition, the average jump size is small compared to the size of the cage, such that the cage trajectory is more or less continuous for PEO, whereas for PMMA it is discrete. Mobility of PMMA should be properly treated by a jump diffusion model, whereas for PEO, a continuous diffusion model is appropriate. We can thus define three types of mobility within the segmental region, depending on the local cage size and the spatial region investigated: motion within a single cage [cage rattling], motion with a spatial extent larger than the cage size where the cages are not overlapping [jump diffusion], and motion with a spatial extent larger than the cage size with overlapping cages [continuous diffusion]. The fact that the cage size is so large for PEO has two effects: the fast decay corresponding to cage rattling is unusually prominent, as seen in Figure 9, and a jump diffusion region is never observed. It is unclear why the idea of a local concentration at a single length scale fails for continuous diffusion. It may be that the intermingling of PEO atoms results in a local concentration that fluctuates and evolves far more rapidly than the time interval required for dynamic decay, such that during this time many different atoms have visited the investigated area and one must take all of them into account when assigning dynamic behavior.

Interpretation in Terms of a Single Dynamic Length Scale. We have observed that both PEO and PMMA, when mixed by forming a diblock copolymer instead of a blend, have lower effective concentrations over length scales surrounding their Kuhn lengths. This influences dynamics, as assessed by segmental relaxation times, in the expected way: the lower effective concentration leads to a larger influence from the mixture partner. For PMMA, this influence is independent of spatial scale, as would be expected on the basis of a single controlling length scale for dynamics. For PEO, differences independent of spatial scale are observed over regions of size less than ~7 Å. We now examine whether the chain connectivity picture is able to describe differences between the copolymer and blend systems. If so, the effective concentration at the Kuhn length of each species should lead to an accurate prediction of the change in dynamics at all length scales.

To provide a numerical value for the segmental relaxation time of either component in the mixed states, $\tau_{seg}^{A}(\phi,T)$, we require the pure component Vogel parameters B_i and τ_∞. As pure component values are used for this purpose, they are the same in both the blend and the copolymer. We use the pure component Vogel parameters T_0 and B_i reported in ref 19 for PEO and in ref 42 for PMMA. We do not require values of τ_∞ because we report the ratio of blend to copolymer relaxation times. Rather than use predicted values of the self [and thus effective] concentrations of PEO and PMMA, we use the effective concentrations determined directly from the simulations at the Kuhn length of each component. This set of parameters is used to predict the ratio $\tau_{blend}/\tau_{copolymer}$ as a function of spatial scale. Because the effective concentration is assigned at a single spatial scale, the chain connectivity model predicts that the ratio of relaxation times is invariant: a plot of $\tau_{blend}/\tau_{copolymer}$ vs Q yields a flat line with a value controlled by the difference in $\phi_{eff,copolymer}$ and $\phi_{eff,\ blend}$. Choosing a value near, but not exactly equal to, the Kuhn length would yield a different value for this ratio, but the plot will remain invariant. In contrast, the ratio obtained from fitting the decay in $F(Q,t)$ to the KWW function and extracting characteristic times has no such restriction.

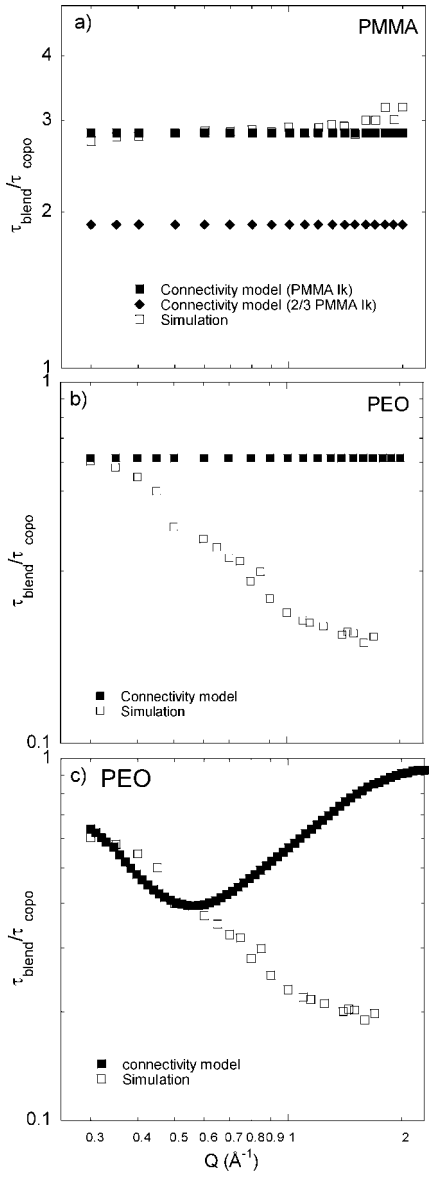

Figure 13. Correlation between measured relaxation times and the prediction of the chain connectivity model. Measured and predicted values of the ratio τ_{blend}/τ_{copo} are presented for (a) PMMA (squares) using the effective concentration at the Kuhn length for all spatial scales and (diamonds) using the effective concentration at $^2/_3 l_k$, (b) PEO using the effective concentration at the Kuhn length for all spatial scales, and (c) PEO using the effective concentration corresponding to the spatial scale of the measurement $\phi_{eff}(r = 2\pi/Q)$. Unfilled symbols: ratio obtained from fitting simulation decay curves. Filled symbols: values predicted by the connectivity model.

The comparison between these two methods of determining the ratio of relaxation times—the prediction of the chain connectivity model and measurement from simulated decay curves—is presented in Figure 13. For PMMA, the prediction of the model is quantitatively accurate, confirming that the idea of a single controlling length scale for dynamics, combined with the concept of a local concentration that varies from the bulk provides an excellent physical picture. We note that the agreement at the exact value of the Kuhn length is perhaps fortuitous. We use spherical volume of diameter equal to the Kuhn length, which corresponds to the volume of a cube with side $0.52 l_k$, close to that found in a recent investigation of PEO/PMMA homopolymer blends.[43] In this reference, T_gs from DSC experiments were described using a self concentration corresponding to a length scale of about two-thirds of the Kuhn length.

The situation for PEO is different. As may be anticipated on the basis of Figure 13b, the measured values of blend and copolymer relaxation times result in a ratio that varies smoothly with spatial scale, in contrast to the prediction of the chain connectivity model. At the largest spatial scales of our calculations [∼21 Å], the prediction quantitatively agrees with the measured changed in relaxation times. The measured change quickly decreases from this value; in the region where the ratio $\tau_{blend}/\tau_{copolymer}$ is relatively flat [$Q > 1$ Å^{-1}], the magnitude of the change is much larger than the effective concentrations at the Kuhn length of PEO predict. Another option for the prediction is to take into account the variation of effective concentration with spatial scale, by using the measured effective concentration corresponding to each Q value, as opposed to the Kuhn length. We have recalculated the chain connectivity prediction in this way, and the results are presented in Figure 13c. This procedure improves things somewhat: reasonable correspondence is observed up to $Q \sim 0.6$ [length scales above 10.5 Å]. At length scales smaller than this, the observed difference in relaxation times is larger than that predicted by the relative effective concentrations at any length scale. This may be a reflection of the direct influence of the junction point in the copolymer, which for PEO we were unable to ascertain and remove from the comparison. Since the qualitative ideas behind this model appear accurate for PEO, copolymer relaxation times are slower; in keeping with the decreased effective concentration of PEO and corresponding increased influence of PMMA, this possibility is likely. Even in that case, differences between the two components are apparent: within the spatial range where agreement can be found, the relevant length scale for dynamics appears to vary for PEO, whereas a single length scale is appropriate for PMMA.

We have considered various possibilities for the length scale over which the effective concentration must be defined to describe the difference in PEO dynamics between the copolymer and blend systems. Using a single controlling length scale of the Kuhn length does not explain the data, nor does assuming the controlling length scale equals measurement length scale, defined by $r_m = 2\pi/Q$. The latter improves the situation but also does not describe all of the data. Now we ask what variation in controlling length scale is required to explain our results. To do this, we determine the effective concentration needed to describe the ratio τ_{blend}/τ_{copo}, at each measurement length scale, r_m. We then assign the controlling length scale, r_c, as the one where the effective concentration takes the required value. These two length scales are plotted against one another in Figure 14, which reveals the surprising feature that as the length scale of the measurement is decreased, the controlling dynamic length scale increases. If the PEO atoms explore large regions [$r_m >$ 16], the Kuhn length is the appropriate dynamic length scale. When the atoms explore small regions [$r_m < 5$], a different length scale [∼5 Å] is appropriate. The appearance of this region is consistent with the analysis surrounding Figure 14. The local cage size for PEO is ∼5 Å, a value larger than other polymers, including PMMA. For measurement length scales within a single cage, the cage size is the appropriate controlling dynamic length scale. The unusual behavior for PEO thus appears to be a combination of a small Kuhn length and a large cage size.

Concluding Remarks

The objective of this work was to examine segmental dynamics as a function of effective concentration leaving all other variables constant. To accomplish this objective, we constructed two systems, both comprised of 20 wt % PEO and 80 wt % PMMA: a blend of the two homopolymers and a diblock copolymer. The different natures of these two mixtures results in different effective concentrations, originating from

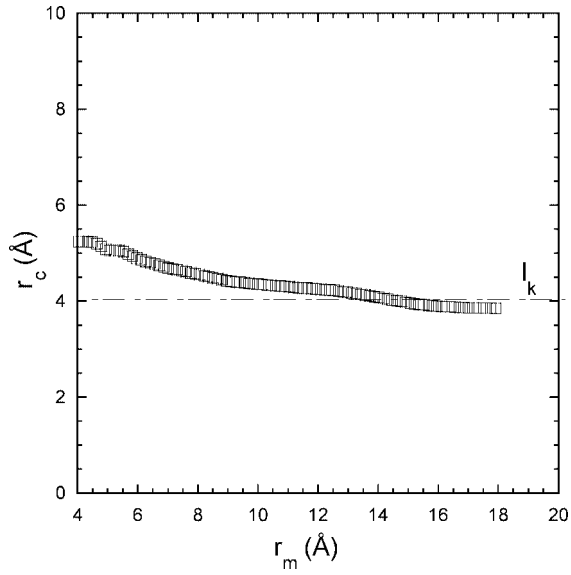

Figure 14. Size of the length scale over which the effective concentration must be defined [controlling dynamic length scale, r_c] as a function of the length scale of measurement, r_m, for the PEO component.

differences in intermolecular packing. For the PMMA component, the change in effective concentrations at the Kuhn length provides an excellent description of the associated change in dynamics, when analyzed with the chain connectivity model. This result emphasizes several physical features about this model: the idea of a local concentration that differs from the bulk and defines dynamic response, the size of this "dynamic bead" being the Kuhn length, and the concept of a single controlling length scale for dynamics. Our simulations were done at a single temperature, so we cannot comment on whether this length scale would be temperature dependent. In obtaining this correlation, we removed from consideration any atoms directly influenced by the junction point: although in a high molecular weight system these would have little influence, in the low molecular weight system that we simulate they could shift the results in an observable manner.

The PEO component does not follow the physical features of the chain connectivity model throughout the spatial range investigated. Although the concept of a local composition appears accurate, both the concept of a single controlling volume for dynamics and the size of that volume being associated with the Kuhn length do not describe our results. Instead, the controlling volume for dynamics is equal to the Kuhn length when the measurement length scale encompasses multiple local cage sizes. When the size of the measured region is within one local cage, it is the cage size that controls dynamics. This behavior is prominent in PEO because its cage size is large enough to overlap both the typical measurement range for the self intermediate scattering function and the Kuhn length.

Finally, we comment that intermolecular packing and thus effective concentrations on local length scales change significantly when going from a blend to a copolymer. In contrast to changes due to thermodynamic fluctuations, this change will be independent of molecular weight and should be taken into consideration when measurements are made on copolymer systems in order to measure systems that would not be miscible as a blend. These systems may behave differently than the corresponding blends, with values of ϕ_{self} different than those for the same component in blends.

Acknowledgment. We gratefully acknowledge the financial support of the Department of Energy under Grant DE-FG02-02ER-25535 and the National Science Foundation under Grant DMR-0134910.

References and Notes

(1) Colby, R. H. *Polymer* **1989**, *30*, 1275.
(2) Cendoya, I.; Alegrıa, A.; Alberidi, J. M.; Grimm, J. C. H.; Richter, D.; Frick, B. *Macromolecules* **1999**, *32*, 4065–4078.
(3) Chung, C. C.; Kornfield, J. A.; Smith, S. D. *Macromolecules* **1994**, *27*, 5729.
(4) Roovers, J. E. L.; Toporowski, P. M. *Macromolecules* **1992**, *25*, 1096.
(5) Paul, D. R.; Newman, S. *Polymer Blends*; Academic Press: New York, 1978; Vol. *1*.
(6) Roland, C. M.; Ngai, K. L. *Macromolecules* **1991**, *24*, 2261–2265.
(7) Kamath, S.; Colby, R. H.; Kumar, S. K.; Karatasos, K.; Floudas, G.; Fytas, G.; Roovers, J. E. L. *J. Chem. Phys.* **1999**, *111*, 6121.
(8) Donth, E. *J. Non-Cryst. Solids* **1982**, *53*, 325.
(9) Donth, E. *J. Non-Cryst. Solids* **1991**, *131*, 204.
(10) Lodge, T. P.; McLeish, T. C. B. *Macromolecules* **2000**, *33*, 5278–5284.
(11) Hirose, Y.; Urakawa, O.; Keiichiro, A. *J. Polym. Sci., Part B: Polym. Phys.* **2004**, *42*, 4084–4094.
(12) Neelakantan, A.; Maranas, J. K. *J. Chem. Phys.* **2004**, *120*, 465–474.
(13) Neelakantan, A.; Maranas, J. K. *J. Chem. Phys.* **2004**, *120*, 1617–1626.
(14) Neelakantan, A.; Stine, R.; Maranas, J. K. *Macromolecules* **2003**, *36*, 3721–3731.
(15) Kanetakis, J.; Fytas, G.; Kremer, F.; Pakula, T. *Macromolecules* **1992**, *25*, 3484–3491.
(16) Rizos, A. K.; Fytas, G.; Roovers, J. E. L. *J. Chem. Phys.* **1992**, *97*, 6925–6932.
(17) Doxastakis, M.; Chrissopoulou, K.; Aouadi, A.; Frick, B.; Lodge, T. P.; Fytas, G. *J. Chem. Phys.* **2002**, *116*, 4707–4714.
(18) Lutz, T. R.; He, Y.; Ediger, M. D. *Macromolecules* **2005**, *38*, 9826–9835.
(19) Lutz, T. R.; He, Y.; Ediger, M. D.; Cao, H.; Lin, G.; Jones, A. A. *Macromolecules* **2003**, *36*, 1724–1730.
(20) Okada, O.; Oka, K.; Kuwajima, S.; Toyoda, S.; Takanabe, K. *Comput. Theor. Polym. Sci.* **2000**, *10*, 371.
(21) Smith, G. D.; Jaffe, R. L.; Yoon, D. Y. *J. Phys. Chem.* **1993**, *97*, 12752.
(22) Chen, C. X.; Depa, P.; García, S., V.,; Maranas, J. K.; Lynn, J. W.; Peral, I.; Copley, J. R. D. *J. Chem. Phys.* **2006**, *23*, 234901.
(23) Chen, C. X.; Maranas, J. K.; Garcían Sakai, V. *Macromolecules* **2006**, *39*, 9630–9640.
(24) Berendsen, H. J. C.; Postma, J. P. M.; Van Gunsteren, W. F. A.; Di Nola Haak, J. R. *J. Chem. Phys.* **1984**, *81*, 3684.
(25) Genix, A. C.; Arbe, A.; Colmenero, J.; Willner, L.; Richter, D. *Phys. Rev. E* **2005**, *72*, 031808–20.
(26) Ewald, P. P. *Ann. Phys.* **1921**, *64*, 253.
(27) Ewald, P. P. *Macromol. Theory Simul.* **1980**, *23*, 3456.
(28) Humphreys, D. D.; Friesner, R. A.; Berne, B. J. *J. Phys. Chem.* **1994**, *98*, 6885.
(29) Tuckerman, M.; Berne, B. J.; Martyna, G. J. *J. Chem. Phys.* **1992**, *97*, 1990.
(30) Mark, J. E. *Physical Properties of Polymers Handbook*; AIP Press Woodbury, NY, 1996.
(31) Zorn, R.; Arbe, A.; Colmenero, J.; Frick, B.; Richter, D.; Buchenau, U. *Phys. Rev. E* **1995**, *52*, 781.
(32) Colmenero, J.; Arbe, A.; Frick, B.; Mijangos, C.; Reinecke, H. *Phys. Rev. E* **1997**, *78*, 1928.
(33) He, Y.; Lutz, T. R.; Ediger, M. D. *J. Chem. Phys.* **2003**, *119*, 9956.
(34) Neelakantan, A.; May, A.; Maranas, J. K. *Macromolecules* **2005**, *38*, 6598–6609.
(35) Williams, G.; Watts, D. C. *Trans. Faraday Soc.* **1970**, *66*, 80.
(36) Bennemann, C.; Baschnagel, J.; Paul, W. *Eur. Phys. J. B* **1999**, *10*, 323.
(37) Wuttke, J.; Chang, I.; Randall, O. G.; Fujara, F.; Petry, W. *Phys. Rev. E* **1996**, *54*, 5364.
(38) Arbe, A.; Colmenero, J.; Monkenbusch, M.; Richter, D.; Farago, B.; Frick, B. *Phys. Rev. E* **2002**, *89*, 245701.
(39) Depa, P. K.; Maranas, J. K. *J. Chem. Phys.* **2007**, *126*, 054903.
(40) Harmandaris, V. A.; Mavrantzas, V. G.; Theodorou, D. N.; Kröger, M.; Ramirex, J.; Ottinger, H. C.; Vlassopoulos, G. *Macromolecules* **2003**, *36*, 1376.
(41) Harmandaris, V. A.; Mavrantzas, V. G.; Theodorou, D. N. *Macromolecules* **1998**, *31*, 7934–7943.
(42) He, Y.; Lutz, T. R.; Ediger, M. D. *J. Chem. Phys.* **2003**, *119*, 9956–9965.
(43) Lodge, T. P.; Wood, E. R.; Haley Jeffrey, C. *J. Polym. Sci., Part B: Polym. Phys.* **2006**, *44*, 7.

MA8003373